# Controlled synthesis of calcium carbonate in a mixed aqueous solution of PSMA and CTAB

Jiaguo Yu[a,*], Xiufeng Zhao[a,b], Bei Cheng[a], Qingjie Zhang[a]

[a]State Key Laboratory of Advanced Technology for Material Synthesis and Processing, Wuhan University of Technology, No. 122, Luoshi Road, Wuhan City, Hubei Province 430070, PR China
[b]Department of Chemical Engineering, Changji University, Changji 831100, PR China

## Abstract

A mixed system of poly (styrene-alt-maleic acid) (PSMA) and cetyltrimethylammonium bromide (CTAB) was used as a very effective crystal growth modifier to direct the controlled synthesis of $CaCO_3$ crystals with various morphologies and polymorphs. The as-prepared products were characterized with scanning electron microscopy and X-ray diffraction. It was found that the concentrations and relative ratios of PSMA and CTAB in the mixed aqueous solution were turned out to be important parameters for the morphology and polymorph of $CaCO_3$ crystals. Various morphologies of $CaCO_3$ crystals, such as hollow microsphere, peanut and so on, were produced depending on the concentrations and relative ratios of PSMA and CTAB. Moreover, the formation mechanisms of $CaCO_3$ crystals with different morphologies were discussed.
© 2005 Elsevier Inc. All rights reserved.

## 1. Introduction

In the past decade, many efforts have been devoted to the controlled synthesis of inorganic and inorganic/organic hybrid materials with specific size, shape, orientation, morphology, organization, complex form, and hierarchical structure owing to the importance and potential to design new materials and devices in various fields such as catalysis, medicine, electronics, ceramics, pigments, cosmetics, etc. [1–6]. Biological systems are able to generate crystalline materials (e.g., seashells, born, teeth, and many others) with complex morphologies and specific functions at ambient temperature via biomineralization, and biomineralization process is elaborately controlled by some biomacromolecules such as proteins and polysaccharides as crystal growth modifiers [7–10]. The strategy of using organic templates or modifiers with complex functionalization patterns to control the nucleation, growth, and alignment of inorganic crystals has been widely adapted for the biomimetic synthesis of inorganic materials with complex form.

For biomimetic synthesis, one approach is to mimic natural biomineralization processes directly in vitro experiments in the presence of biomacromolecules synthesized or isolated from biological systems [11–16], and another is just to mimic the biomineralization principles, in which synthetic polymers and/or surfactants are used as templates or crystal growth modifiers to control the growth of crystals [17–22].

Recently, new functional polymers, the so-called double-hydrophilic block copolymers (DHBCs) have been developed as novel crystal growth modifiers [1,3]. These copolymers consist of one hydrophilic block designed to interact strongly with the appropriate

---

*Corresponding author. Fax: +86 27 8788 2395.
E-mail address: jiaguoyu@yahoo.com (J. Yu).

inorganic mineral crystal surfaces, and another hydrophilic block that does not interact (or only weakly) with mineral crystal surfaces and mainly promotes solubilization in water. Owing to the separation of the binding and the solvating moieties, these polymers turned out to be extraordinarily effective in crystallization control for various inorganic materials [1,3,4,23]. Notably, inorganic materials with unusual morphologies were also achieved by using the mixed systems of polymer and surfactant as crystal modifiers due to the polymer-surfactant complexes with more complicated structures in aqueous solution showing effective control for the crystallization of inorganic materials [24,25].

In this work, $CaCO_3$ crystals with diverse morphologies and crystal polymorphs were prepared by a simple precipitation reaction of calcium chloride and sodium carbonate at room temperature using a mixed system of poly (styrene-alt-maleic acid) (PSMA) and cetyltrimethylammonium bromide (CTAB) as a effective crystal growth modifier. The as-prepared products were characterized with scanning electron microscopy (SEM) and X-ray diffraction (XRD).

## 2. Experimental

### 2.1. Preparation

PSMA (sodium salt, 30 wt% aqueous, average molecular weight ca. 120000), was purchased from Aldrich, and used without further treatment. All other chemicals, calcium chloride, sodium carbonate, and CTAB used in the experiments were of analytical grade, and the water used in this work was distilled water.

The precipitations of $CaCO_3$ were carried out in glass beakers at room temperature (ca. 22 °C). Aqueous solutions of $Na_2CO_3$ (0.5 M) and $CaCl_2$ (0.5 M) were first prepared as stock solutions. In a typical synthesis, 1.5 mL $CaCl_2$ (0.5 M) solution was added into 97 mL mixed aqueous solution of PSMA and CTAB, and no effort was made to adjust the pH of the mixed solution. After that, equal volume (1.5 mL) of $Na_2CO_3$ solution (0.5 M) was injected into the above solution under vigorous stirring using a magnetic stirrer. The total volume of the working solution was 100 mL, and the final $CaCO_3$ concentration was about 7.5 mM. In all cases, PSMA concentration was kept at 0.5 or 1.5 g/L, the CTAB concentrations varied from 0.2 to 5 mM and starting pH was about 10. After stirring for 1 min, the precipitate was allowed to stand in its mother solution for 24 h before collecting it for characterization. As reference experiments, the $CaCO_3$ precipitations were also produced in the presence of only PSMA, or only CTAB, or no additive, all other conditions being equal.

### 2.2. Characterization

The resulting $CaCO_3$ precipitates were characterized by SEM (type JSM-5610LV) with an accelerating voltage of 20 kV. The powder XRD patterns were obtained on a HZG41B-PC X-ray diffractometer using $CuK\alpha$ radiation at a scan rate of $0.05°2\theta$ $S^{-1}$. The accelerating voltage and the applied current were 15 kV and 20 mA, respectively.

## 3. Results and discussion

### 3.1. Influence of CTAB on the crystallization of $CaCO_3$

Fig. 1(a) and (b) show SEM images of $CaCO_3$ crystals obtained in the absence of additive (a) and in the presence of 1.0 mM CTAB (b), respectively. It can be seen that rhombohedral crystals with smooth surfaces are obtained in water or in the presence of 1.0 mM CTAB. Corresponding XRD results (not shown here) indicate that all the products obtained in the above two cases are pure calcite. It can be concluded that CTAB has no obvious effect on the morphology and
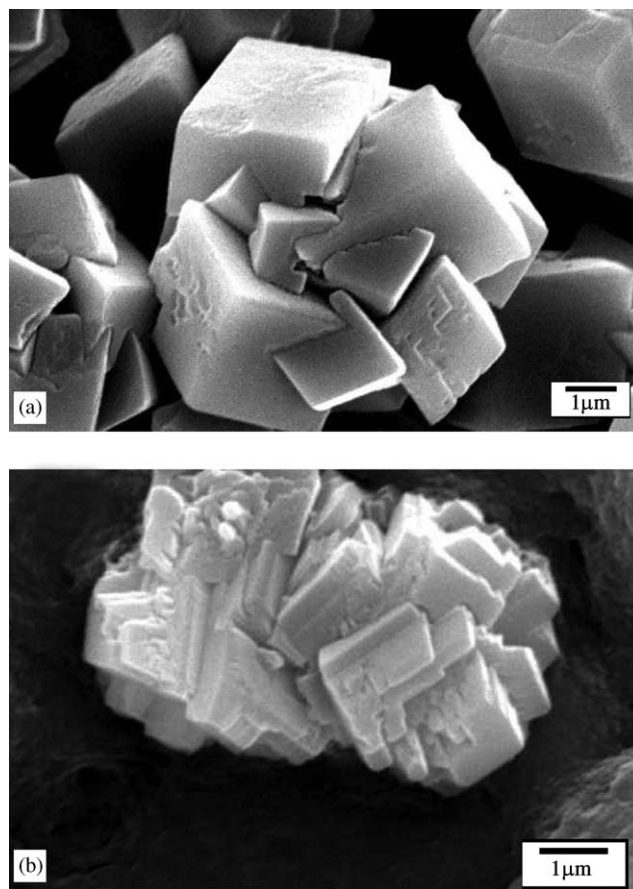


Fig. 1. SEM images of $CaCO_3$ crystals obtained in the absence of additive (a) and in the presence of 1.0 mM CTAB (b).

polymorph of $CaCO_3$ crystals at room temperature. This result is also in agreement with our previous work [26].

## 3.2. Influence of PSMA on the crystallization of $CaCO_3$

Fig. 2 (a) and (b) show SEM images of $CaCO_3$ crystals obtained in the presence of 0.5 and 1.5 g/L PSMA, respectively. At the PSMA concentration of 0.5 g/L, rhombohedra crystals with rugged surfaces were obtained. Further observation shows that many smaller crystals are attached on the surfaces of large crystals (Fig. 2(a)). It can be seen that the morphologies of these $CaCO_3$ crystals are similar to those of the products obtained in water (Fig. 1(a)). Corresponding XRD pattern (Fig. 3(a)) exhibits obvious diffraction peaks from vaterite in addition to the sharp diffraction peaks from calcite, suggesting that the products obtained in the presence of 0.5 g/L PSMA consist of calcite and vaterite and their relative mass percent is about 31% and 69% for calcite and vaterite, respectively. When PSMA concentration was further increased to 1.5 g/L, smaller dumbbell-shaped and pseudo spherical $CaCO_3$ crystals were produced (Fig. 2(b)), which indicated that higher PSMA concentration showed a greater influence
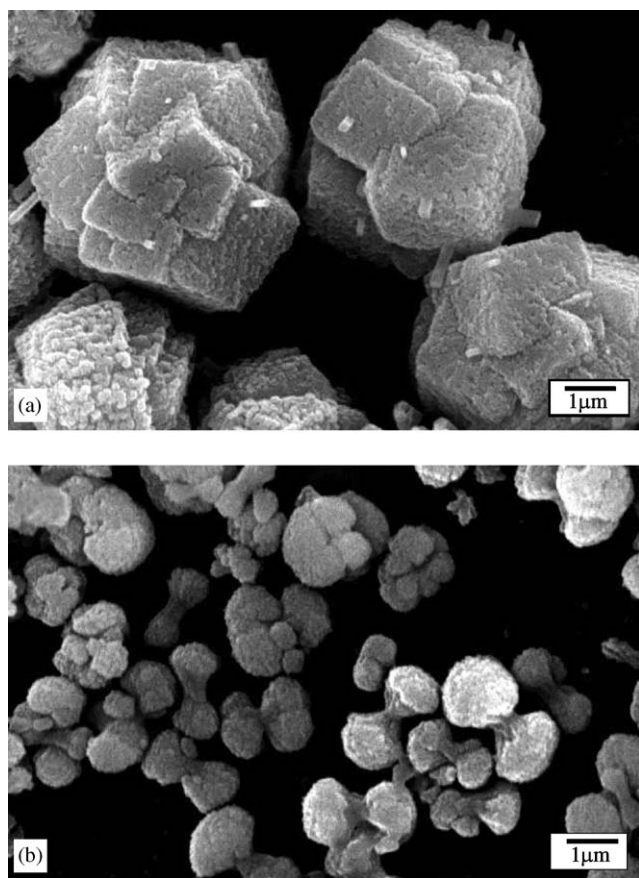


Fig. 2. SEM images of $CaCO_3$ crystals obtained in the presence of 0.5 (a) and 1.5 g/L PSMA (b).
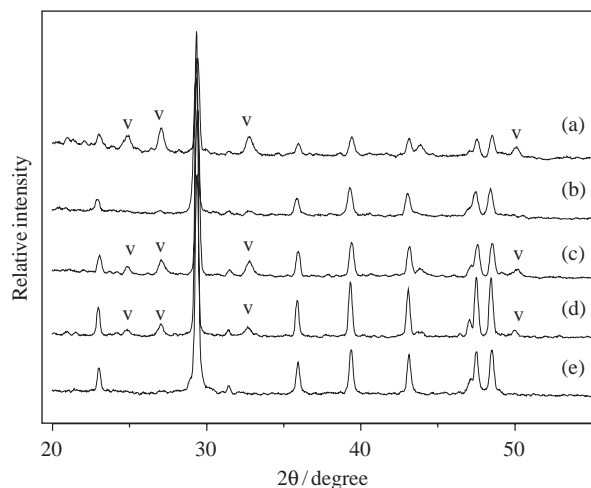


Fig. 3. XRD patterns of $CaCO_3$ crystals obtained in the presence of PSMA and/or CTAB: (a) [PSMA] = 0.5 g/L, (b) [PSMA] = 1.5 g/L, (c) [PSMA] = 0.5 g/L, [CTAB] = 0.5 mM, (d) [PSMA] = 0.5 g/L, [CTAB] = 1.0 mM, (e) [PSMA] = 1.5 g/L, [CTAB] = 0.5 mM. "V" denotes peaks from vaterite.

on the growth and morphology of $CaCO_3$ crystals. XRD result (Fig. 3(b)) suggests that the $CaCO_3$ crystal obtained in the presence of 1.5 g/L PSMA consist of pure calcite. This indicates that low PSMA concentrations favor the formation of vaterite, as previously observed by Colfen at low concentrations of PEG-b-PMAA [1]. It should be noted that there is a significant difference between the current results and our previous results reported in Refs. [2,22,27]. This is ascribed to the fact that their experiment methods and conditions are different.

## 3.3. Influence of PSMA–CTAB mixed system on the crystallization of $CaCO_3$

Fig. 4 shows SEM images of $CaCO_3$ crystals obtained in the presence of 0.5 g/L PSMA and various CTAB concentrations. When CTAB concentration was 0.2 mM in the mixed solution, the morphology of $CaCO_3$ crystals was similar to that of the products produced in the presence of the same PSMA concentration and without CTAB (see Figs. 4(a) and 2(a)). XRD result of this sample shows that the $CaCO_3$ powders also contain calcite and vaterite. It can be concluded from the above results that a small amount of CTAB in the mixed solution has no obvious influence on the morphology and polymorph of $CaCO_3$ crystals. When the CTAB concentration was increased to 0.5 mM, the morphology of $CaCO_3$ crystals was similar to that of the products obtained at a CTAB concentration of 0.2 mM, but their surface roughness slightly reduced (see Fig. 4(a) and (b)). XRD pattern shown in Fig. 3(c), however, reveals that these crystals are composed of calcite and vaterite and their relative mass percent is about 76% and 24%,
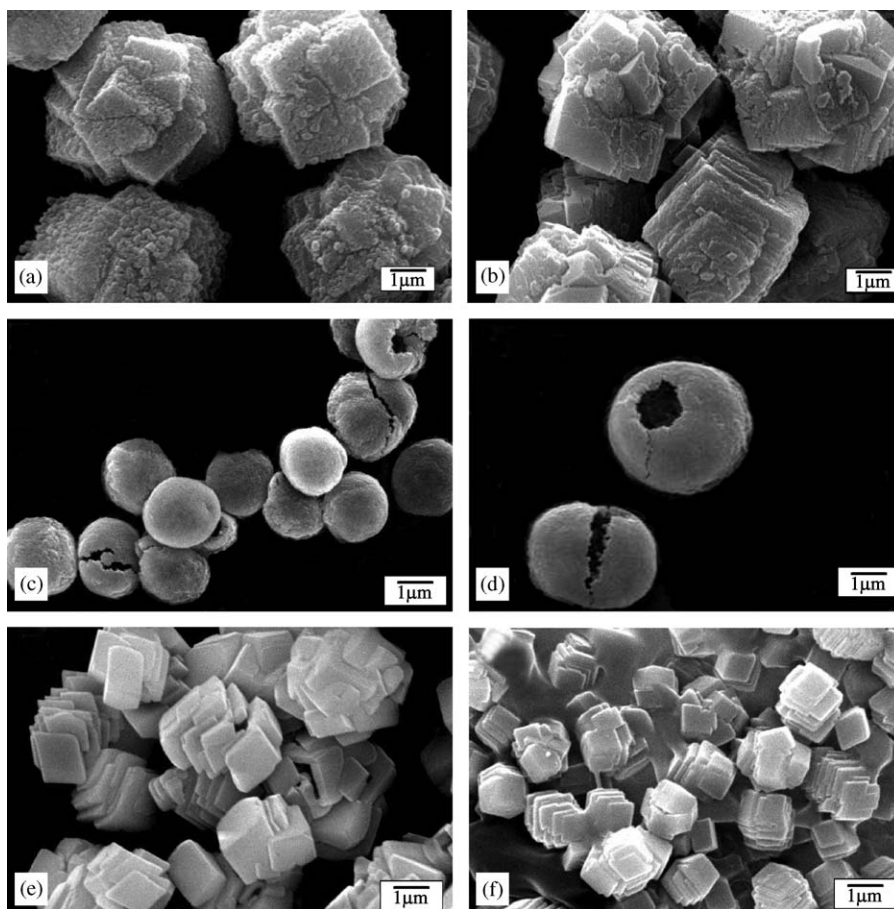
Fig. 4. SEM images of CaCO$_3$ crystals obtained in the presence of 0.5 g/L PSMA and (a) 0.2, (b) 0.5, (c and d) 1.0, (e) 1.5 and (f) 5.0 mM CTAB.

respectively. Interestingly, when CTAB concentration was increased to 1 mM, well-defined CaCO$_3$ hollow spherical crystals were obtained and the particle size was about 2–3 μm (Fig. 4(c) and (d)). Fig. 4(d) shows a high-magnification SEM image of two broken microspheres, which exhibit rough surfaces and the morphological feature of hollow microspheres. The XRD investigation shows that hollow CaCO$_3$ microspheres consist of 96% calcite and 4% vaterite (Fig. 3(d)). When the CTAB concentration was further increased to 1.5 or 5.0 mM, rhombohedral CaCO$_3$ crystals were obtained (Fig. 4(e) and (f)), and these products consisted of pure calcite. These results indicate that when CTAB concentration is higher than 1.5 mM in the PSMA–CTAB mixed solution, the morphology control of CaCO$_3$ crystals is lost and vaterite phase completely disappears.

The above experimental results could be explained according to the electrostatic interaction between cationic surfactant CTAB and polyanionic electrolyte PSMA in the mixed solutions (Fig. 5). PSMA exhibited obvious influence on the morphology and polymorph of CaCO$_3$ crystals due to the strong interaction between carboxylic acid groups of PSMA and CaCO$_3$ crystal surfaces. However, the interaction between PSMA and
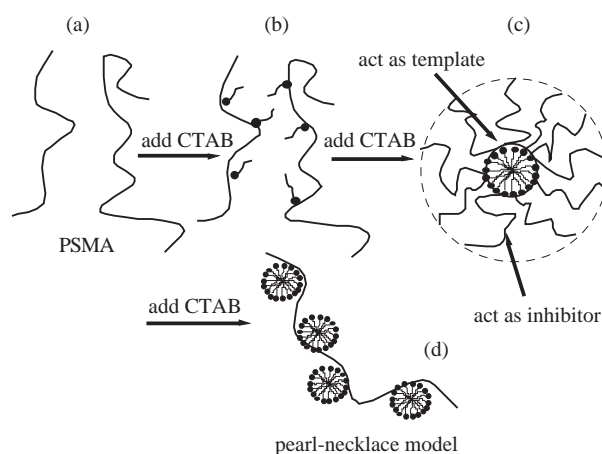


Fig. 5. Schematic model of the electrostatic interaction between cationic surfactant CTAB and polyanionic electrolyte PSMA in water: (a) PSMA molecules in water. (b) CTAB associating to PSMA chains. (c) Several PSMA chains associating to a spherical CTAB micelle. (d) Many spherical CTAB micelles associating to a PSMA chain.

CaCO$_3$ could be reduced by the addition of cationic surfactant CTAB in the solutions. When CTAB concentration was increased to 0.5 mM, the effects of

PSMA on the morphology of $CaCO_3$ crysrals were partially lost. Especially, when CTAB concentration in the mixed solution reached to 1 mM, it was reasonable to assume that the CTAB micelles would firstly form due to the fact that critical micelle concentration (CMC) of CTAB is about 0.92 mM [28]. Then the chains of PSMA were associated to the CTAB micelles to form larger complex micelles due to the strong electrostatic interaction between the cationic polar head groups on the surface of the CTAB micelles and the ionized carboxylic acid groups of PSMA. Probably, for a single PSMA chain, part of the chain was associated to a CTAB micelle, and another was free in the mixed solution. Thus, some carboxylic acid groups on the associated chains were oriented outward due to steric hindrance. Hence, it could be assumed that core-shell micelles could be formed by CTAB micelles as cores and associated PSMA as shells. Such core-shell micelles, the CTAB micelles bound by PSMA chains, would act as the spherical templates. Meanwhile, the free part of PSMA chains in the solution would act as the inhibitors. The cooperative effect of the spherical templates and the inhibitors would finally lead to the formation of $CaCO_3$ hollow spheres around the PSMA–CTAB complex micelles. When CTAB concentration was higher than 1.5 mM, the "pearl-necklace model" [28] of polymer-surfactant association would probably be formed. In this case, a large amount of CTAB micelles were associated to a PSMA chain due to electrostatic interaction, and the interaction between PSMA and $CaCO_3$ crystal surfaces was impaired. Therefore, PSMA gradually lost its control ability to the morphology of $CaCO_3$ crystals.

In order to further investigate the influence of concentrations and relative ratio of PSMA and CTAB on $CaCO_3$ crystallization, another set of experiment was curried out, where PSMA concentration was kept at a higher concentration of 1.5 g/L, the CTAB concentration varied from 0.5 to 1 mM, and all other experimental conditions were kept the same. When PSMA and CTAB concentration were 1.5 g/L and 0.5 mM, respectively, novel peanut-like $CaCO_3$ crystals with rugged surfaces were obtained (Fig. 6(a) and (b)), and XRD result suggested that these crystals consisted of calcite (Fig. 3(e)). These peanut-like crystals clearly showed $1\bar{1}0$ calcite faces at the out range in a staggered prismatic arrangement, reminiscent of the $CaCO_3$ crystals obtained in the presence of a double hydrophilic block copolymer [29]. These $1\bar{1}0$ calcite faces were not expressed in the absence of additive. Generally, all $\alpha$, $\omega$-dicarboxylic acids $(CH_2)_n(CO_2H)_2$ with ionized carboxylic acid groups and $n < 3$ were found to stabilize the $1\bar{1}0$ calcite crystal faces [30]. Hence, it was not too surprising that three-dimension body with expressed $1\bar{1}0$ calcite faces could be obtained in the presence of PSMA. Compared with Fig. 2(b), it seems that the
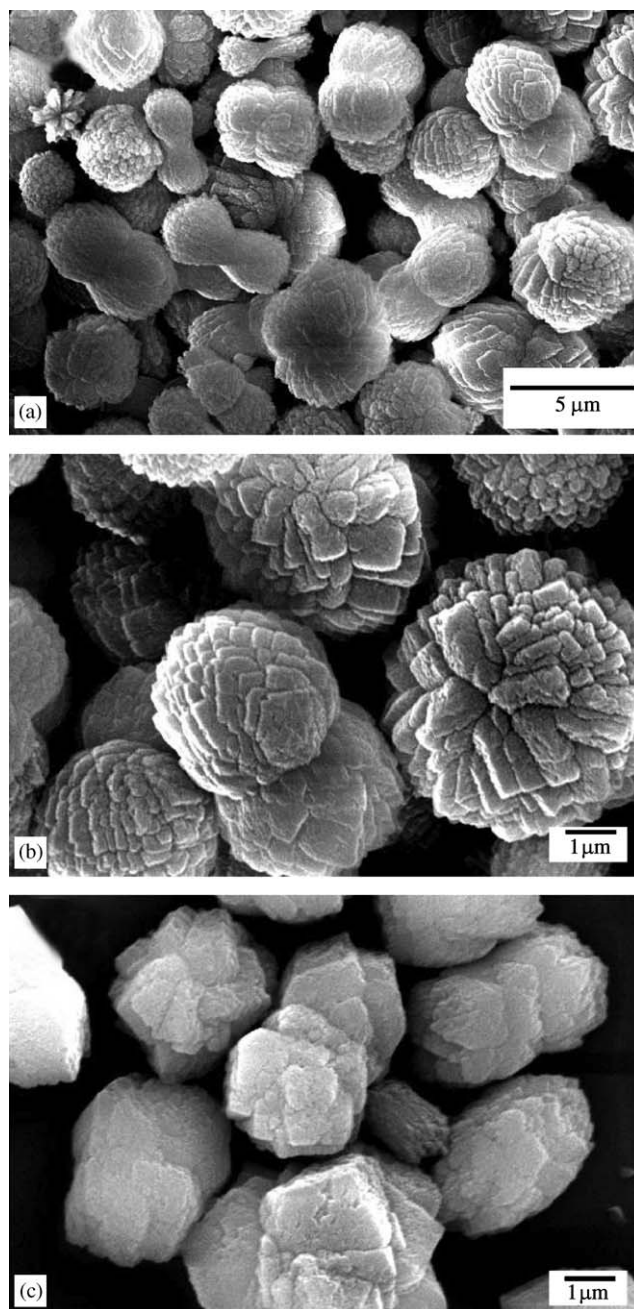


Fig. 6. SEM images of $CaCO_3$ crystals obtained in the presence of 1.5 g/L PSMA and (a) and (b) 0.5 and (c) 1.0 mM CTAB.

presence of 0.5 mM CTAB in the mixed solution weakens the interaction between the PSMA and crystals, resulting in an enhanced selective adsorption of PSMA molecules on $CaCO_3$ crystal faces. In other words, PSMA molecules could adsorb preferentially on the $1\bar{1}0$ calcite faces in the presence of 0.5 mM CTAB in the mixed solution. Hence, these adsorbed PSMA molecules on $1\bar{1}0$ calcite faces directed the crystal growth along the direction parallel to $1\bar{1}0$ faces. This resulted in the staggered sheet-like crystals expressing the $1\bar{1}0$ calcite faces. However, when CTAB concentration was further
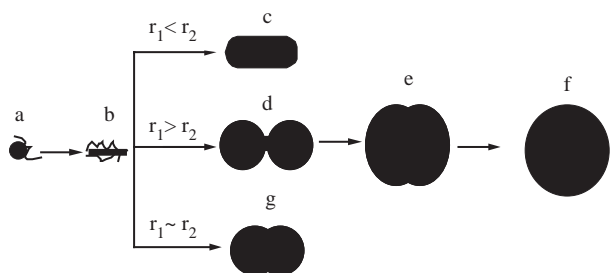
Fig. 7. Schematic illustration of a possible mechanism for twinned morphological formation: (a) Nucleation and growth of amorphous nanoparticles in the PSMA–CTAB mixed solution. (b) Crystallization of an elongated crystal. (c) Formation of rod-like crystals. (d, e and f) Formation of dumbbell-like, notched spherical and spherical crystals. (g) Formation of peanut-like crystals. "$r_1$" and "$r_2$" denote the rate of nucleation and growth outward at the ends of rod-like primary crystals and the rate of nucleation and growth along the rod axes of rod-like primary crystals, respectively.

increased to 1 mM, irregular shaped calcite crystals showing faceted surfaces were obtained (Fig. 6(c)), which implied that morphology control was partially lost at such a high CTAB concentration. Compared with the CaCO$_3$ crystals obtained in the presence of 0.5 g/L PSMA and 1 mM CTAB, it could be inferred that a large amount of PSMA in the mixed solution would probably modify the structure of the complex micelles formed by PSMA and CTAB. Thus, no hollow CaCO$_3$ spherical crystals were obtained in the present case.

Notably, twinned morphological inorganic crystals, such as dumbbell and peanut-shaped crystals, have also been produced in different experimental conditions [3,4,26,29]. It was assumed that the carboxylic acid groups of polymer could be preferentially adsorbed on the growing crystal surfaces parallel to a certain crystallographic direction during crystallization, resulting in rod-like primary crystals [4]. The formation mechanism of the dumbbell- or peanut-like shape was explained in terms of nucleation and growth at the both ends of the rod-like primary crystals along electric field lines; and these dumbbell- or peanut-like crystals could further grow into spherical crystals [4]. It was noteworthy that another formation mechanism of twinned morphology based on the probability of nucleation on the side-surfaces of rod-like primary crystals was also proposed [3]. Probably, a better interpretation for the formation mechanism of such twinned morphological crystals is to assume that the two competitive processes play an important role in determining the final morphology. One process is the nucleation and growth outward along the electric field line at both the ends of rod-like primary crystals [4]. Another process is the nucleation and growing along the rod axes at the side-surfaces of rod-like primary crystals. Fig. 7 shows the schematic illustration of a possible mechanism for twinned morphological formation. We speculate that

the twinned morphology is controlled by the relative size of two kinds of rates $r_1$ and $r_2$. Here, $r_1$ and $r_2$ denote the rate of nucleation and growth outward at the ends of rod-like primary crystals and the rate of nucleation and growth along the rod axes of rod-like primary crystals, respectively. When $r_1$ is much smaller than $r_2$, rod-like or ellipsoid crystals will be obtained; when $r_1$ is much larger than $r_2$, dumbbell-like crystals are favored, and these crystals may further grow to notched spheres and spheres; when there is no obvious difference between $r_1$ and $r_2$, the peanut-like crystals may be produced.

## 4. Conclusions

The PSMA–CTAB mixed systems were used as effective crystal growth modifiers to direct the controlled synthesis of CaCO$_3$ crystals with various morphologies and polymorphs. The concentrations and relative ratios of PSMA and CTAB in the PSMA–CTAB mixed systems exhibited significant influence on the morphology and polymorph of the as-obtained CaCO$_3$ products, though CTAB alone had no obvious effect on the crystallization of CaCO$_3$. Various morphologies of CaCO$_3$, such as hollow sphere, peanut and so on, were produced depending on the concentrations and relative ratios of PSMA and CTAB. The interaction between PSMA and crystal surfaces could be adjusted by varying the concentrations and relative ratios of PSMA and CTAB. Probably, the complex micelles with a specific structure formed by PSMA and CTAB could act as the spherical templates and inhibitors simultaneously, resulting in the formation of CaCO$_3$ hollow microspheres. The experimental results also suggested that such mixed systems, with a negatively charged polymer and a cationic surfactant, might be the promising candidates for crystal growth modifiers.

## References

[1] H. Colfen, L.M. Qi, Chem. Eur. J. 7 (2001) 106.
[2] J.G. Yu, J.C. Yu, L.Z. Zhang, X.C. Wang, L. Wu, Chem. Commun. (2004) 2414.
[3] L.M. Qi, H. Colfen, M. Antonietti, Chem. Mater. 12 (2000) 2392.
[4] S.H. Yu, H. Colfen, A.W. Xu, W.F. Dong, Cryst. Growth Des. 4 (2004) 33.

[5] P. Liang, Y. Zhao, Q. Shen, D.J. Wang, D.F. Xu, J. Cryst. Growth 261 (2004) 571.

[6] J.G. Yu, M. Lei, B. Cheng, X.J. Zhao, J. Solid State Chem. 177 (2004) 681.

[7] S. Weiner, Crit. Rev. Biochem. 20 (1986) 365.

[8] S. Mann, J. Webb, R.J.P. Williams, Biomineralization, Chemical and Biochemical Perspectives, VCH, Weinheim, 1989.

[9] S. Mann, C.C. Perry, Adv. Inorg. Chem. 36 (1991) 137.

[10] M. Fritz, D.E. Morse, Curr. Opin. Colloid Interface Sci. 3 (1998) 55.

[11] G. Falini, S. Albeck, S. Weiner, L. Addadi, Science 271 (1996) 67.

[12] Y. Levi, S. Albeck, A. Brack, S. Weiner, L. Addadi, Chem. Eur. J. 4 (1998) 389.

[13] A.M. Belcher, X.H. Wu, R.J. Christensen, P.K. Hansma, G.D. Stuky, D.E. Morse, Nature 381 (1996) 36.

[14] D.B. DeOliveira, R.A. Laursen, J. Am. Chem. Soc. 119 (1997) 10627.

[15] G. Falini, S. Fermani, M. Gazzano, A. Ripamonti, Chem. Eur. J. 3 (1997) 1807.

[16] G. Falini, S. Fermani, M. Gazzano, A. Ripamonti, Chem. Eur. J. 4 (1998) 1048.

[17] S. Mann, B.R. Heywood, S. Rajam, S.J.D. Birchall, Nature 334 (1988) 692.

[18] J.M. Didymus, S. Mann, W.J. Benton, I.R. Collins, Langmuir 11 (1995) 3130.

[19] A.L. Litvin, S. Valiyaveettil, D.L. Kaplan, S. Mann, Adv. Mater. 9 (1997) 124.

[20] R.J. Davey, S.N. Black, L.A. Bromley, D. Cotter, B. Dobbs, J.E. Rout, Nature 353 (1991) 549.

[21] J.M. Didymus, P. Oliver, S. Mann, A.L. DeVries, P.V. Hauschka, P. Westbroek, J. Chem. Soc. Faraday Trans. 89 (1993) 2891.

[22] J.G. Yu, J.C. Yu, Key Eng. Mater. 280–283 (2005) 601.

[23] M. Sedlak, M. Antonietti, H. Colfen, Macromol. Chem. Phys. 199 (1998) 247.

[24] L.M. Qi, J. Li, J.M. Ma, Adv. Mater. 14 (2002) 300.

[25] H. Wei, Q. Shen, Y. Zhao, D.J. Wang, D.F. Xu, J. Cryst. Growth 264 (2004) 424.

[26] J.G. Yu, M. Lei, B. Cheng, X.J. Zhao, J. Cryst. Growth 261 (2004) 566.

[27] N. Spanos, P.G. Koutsoukos, J. Cryst. Growth 191 (1998) 783.

[28] K. Holmberg, B. Josson, B. Kronberg, B. Lindmann, Surfactants and Polymers in Aqueous Solution, Wiley, New York, 2002.

[29] H. Colfen, M. Antonietti, Langmuir 14 (1998) 582.

[30] S. Mann, Biomineralization Principles and Concepts in Bio-inorganic Materials Chemistry, Oxford Press, New York, 2001, p. 56.